

# Entanglement between deconfinement transition and chiral symmetry restoration

Yuji Sakai<sup>\*†</sup>, Takahiro Sasaki<sup>\*†</sup>, Hiroaki Kouno<sup>‡</sup>, Masanobu Yahiro<sup>†</sup>

Department of Physics, Kyushu University<sup>†</sup>,

Department of Physics, Saga University<sup>‡</sup>,

## 1 Introduction

An important query on the QCD thermodynamics is whether the chiral-symmetry restoration and the deconfinement transition take place simultaneously or not. Actually, in lattice QCD (LQCD) simulations at zero chemical potential ( $\mu_q$ ), there is a debate as to whether the transitions really coincide or not [1]. LQCD simulations are far from perfection at real  $\mu_q$  because of the sign problem. Fortunately, LQCD data are available at imaginary  $\mu_q$  [2] and isospin chemical potential  $\mu_I$  [3], since there is no sign problem. The data show that chiral and deconfinement transitions coincide in the numerical accuracy. Since there is no general reason for coincidence between the two crossover transitions, it is natural to think that the chiral and deconfinement transitions nearly coincide as a result of strong entanglement between the two order parameters: the chiral condensate and the Polyakov loop. We investigate this possibility in the present paper.

## 2 PNJL model

We consider the Polyakov-loop extended Nambu–Jona-Lasinio (PNJL) model which can treat both the chiral and deconfinement transitions. The two-flavor PNJL Lagrangian is

$$\mathcal{L} = \bar{q}(\gamma_\nu D_\nu + m_0)q + G_s[(\bar{q}q)^2 + (\bar{q}i\gamma_5\vec{\tau}q)^2] - \mathcal{U}(\Phi, \Phi^*), \quad (1)$$

where  $q$  denotes the two-flavor quark field,  $m_0$  does the current quark mass, and  $D_\nu = \partial_\nu - iA_\nu\delta_{\nu 4}$ . Here the Polyakov potential  $\mathcal{U}$  [4] is a function of the Polyakov loop  $\Phi = \frac{1}{N_c} \text{tr}_c e^{-iA_4/T}$  and its conjugate  $\Phi^*$ . We take the Polyakov gauge where  $A_4$  can take a diagonal form. The chiral condensate  $\sigma = \bar{q}q$  and the Polyakov loop  $\Phi$  are order parameters for the chiral and deconfinement transitions, respectively. In the mean field approximation,  $\sigma$ ,  $\Phi$  and  $\Phi^*$  satisfy the stationary conditions of the thermodynamic potential. The PNJL model can reproduce the LQCD results at imaginary  $\mu_q$  [5], particularly

<sup>\*</sup>supported by JSPS Research Fellow.

the model has the Roberge-Weiss periodicity that is a periodicity of  $\theta = \text{Im}(\mu_q)/T$  with period  $2\pi/3$ . The RW periodicity is due to invariance under the extended  $\mathbb{Z}_3$  transformation, which is a combination of the  $\mathbb{Z}_3$  transformation and  $\theta \rightarrow \theta + 2\pi/3$ . This symmetry guarantees that the PNJL model can reproduce the LQCD results qualitatively at imaginary  $\mu_q$ . Figure 1 (a) shows the phase diagram of the PNJL model at imaginary  $\mu_q$ . The chiral and deconfinement transitions separate each other by 20 %. The PNJL model reproduces the LQCD results for the deconfinement transition, but not for the chiral transition. This indicates that the entanglement between the chiral and deconfinement transitions is weak in the PNJL model. This problem will be discussed in the next section.

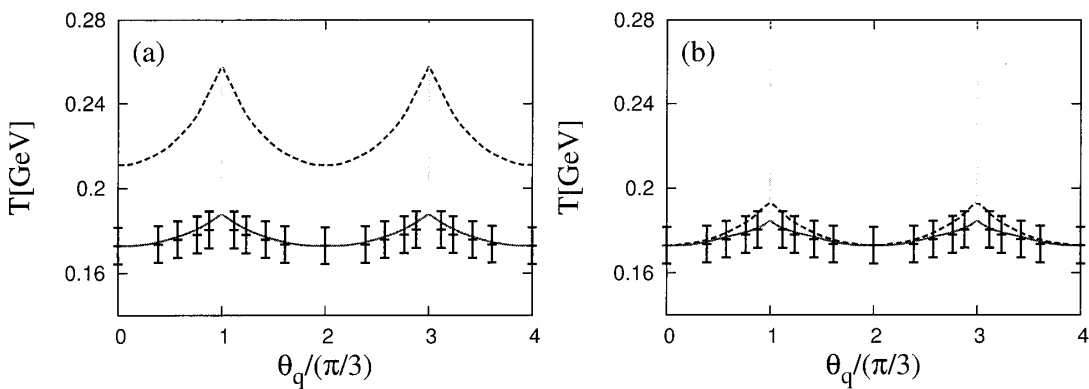


Figure 1: Phase diagram at imaginary chemical potential (a) by the PNJL model and (b) by the EPNJL model. The solid (dashed) lines represent the deconfinement (chiral) transition lines. The vertical dot-dashed lines denote the RW transition lines. Lattice data are taken from Ref. [2].

### 3 Entanglement PNJL model

In the NJL-type model, the four-quark vertex  $G_s$  is originated from the one-gluon exchange between two quarks and its higher-order exchanges. If the gluon field  $A_\nu$  has a vacuum expectation value  $\langle A_4 \rangle$  in its temporal component,  $A_\nu$  is coupled to  $\langle A_4 \rangle$  which is related to  $\Phi$ ; see Fig. 2. Hence,  $G_s$  is changed into an effective (entanglement) vertex  $G_s(\Phi)$  that

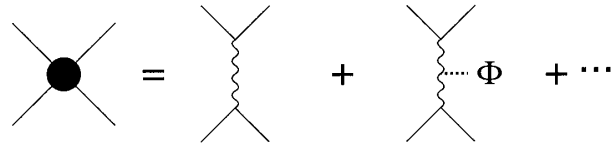


Figure 2: The diagrammatic description of the effective vertex  $G_s(\Phi)$ .

can depend on  $\Phi$  [6]. Actually, recent analyses [6] based on the exact renormalization-group method indicate that entanglement interactions between  $\sigma$  and  $\Phi$  appear in addition to the original entanglement through the covariant derivative. It is expected that the  $\Phi$  dependence of  $G_s(\Phi)$  will be determined in the future by exact renormalization group

method. In this paper, however, we simply assume the following  $G_s(\Phi)$  that preserves chiral symmetry, charge conjugate symmetry and extended  $\mathbb{Z}_3$  symmetry [5]:

$$G_s(\Phi) = G_s[1 - \alpha_1\Phi\Phi^* - \alpha_2(\Phi^3 + \Phi^{*3})]. \quad (2)$$

The PNJL model with the entanglement vertex  $G_s(\Phi)$  is referred to as entanglement PNJL (EPN JL) model. The EPN JL model has entanglement interactions between  $\sigma$  and  $\Phi$  in addition to the covariant derivative in the original PNJL model. Figure 1 (b) shows the phase diagram of the EPN JL model at imaginary  $\mu_q$ . In this model, the two transitions coincide with each other as a consequence of the strong entanglement between  $\sigma$  and  $\Phi$ . Thus, the EPN JL model reproduces the LQCD results at imaginary  $\mu_q$ . Since the EPN JL model is constructed so as to reproduce LQCD data at imaginary  $\mu_q$ , the validity of the model is confirmed for isospin chemical potential where LQCD data are available. As shown in Fig. 3 (a), the EPN JL model also reproduces the LQCD results at isospin chemical potential. Finally we predict the phase diagram in the whole  $\mu_q^2 - T$  plane by using the EPN JL model in Fig. 3 (b). Location of the critical end point (CEP) moves to lower  $\mu_q$  in the EPN JL model than that in the PNJL model.

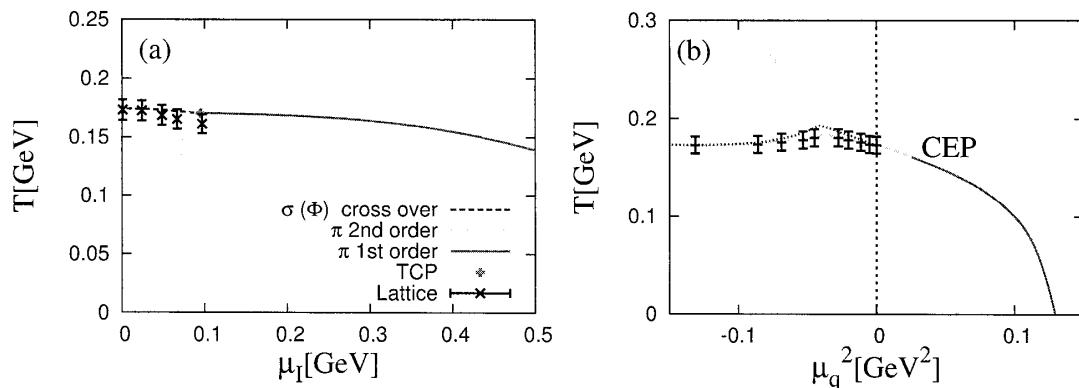


Figure 3: (a) Phase diagram at isospin chemical potential by the EPN JL model. LQCD data are taken from Ref. [3]. (b) Phase diagram in the  $\mu_q^2 - T$  plane in the EPN JL model. The left (right) half-plane corresponds to imaginary (real)  $\mu_q$ . Lattice data are taken from Ref. [2].

## References

- [1] S. Borsányi, et., al. arXiv:1005.3508 [hep-lat] (2010).
- [2] P. de Forcrand and O. Philipsen, Nucl. Phys. **B642**, 290 (2002).
- [3] J. B. Kogut, and D. K. Sinclair, Phys. Rev. D **70**, 094501 (2004).
- [4] S. Rößner, C. Ratti, and W. Weise, Phys. Rev. D **75**, 034007 (2007).
- [5] Y. Sakai, T. Sasaki, H. Kouno, and M. Yahiro, Phys. Rev. D **82**, 076003 (2010).
- [6] K.-I. Kondo, Phys. Rev. D **82**, 065024 (2010).